Two-dimensional nonlocal heating theory of planar-type inductively coupled plasma discharge

N. S. Yoon, S. M. Hwang, and Duk-In Choi*
Korea Basic Science Institute, Taejeon 305-333, Korea
(Received 9 December 1996)

A two-dimensional heating theory of planar-type inductively coupled plasma (ICP) discharge is developed. The theory includes the anomalous skin effect with an arbitrary value of electron collision frequency and source current. Based on the uniqueness theorem of wave equation, wave excitation by the source current is determined. With the calculated electromagnetic fields, plasma resistance is expressed as a function of various parameters such as plasma density n_p, electron temperature T_e, radius of chamber R, length of plasma L_p, shielding cap length L_s, electron collision frequency ν, excitation frequency ω, and the position and size of the antenna coil. [S1063-651X(97)14606-2]

PACS number(s): 52.80.Pi, 52.50.−b, 52.75.−d

I. INTRODUCTION

Inductively coupled plasma (ICP) sources have been the subject of many experimental and theoretical investigations [1–10], owing to the fact that a high-density plasma with good uniformity is easily obtained under low pressure without an external magnetic field. Two types of ICP reactors are available [11], classified according to shape and the position of the coil. One type of reactor has a planar coil at the top of the cylindrical chamber (planar type, also called TCP) [1–9], and the other one has a solenoidal coil wound at the side of the chamber (solenoidal type) [10]. The ICP reactor can be easily scaled up to accommodate a larger wafer size comparing to the other reactors (Helicon, electron cyclotron resonance, etc.) because the system is substantially simpler.

For the electron heating mechanism of ICP discharge, collisionless heating is widely accepted as the primary mechanism on sustaining low-pressure inductive radio-frequency discharges. It has also been suggested, in both planar-type [12] and solenoidal-type [10] reactors, that the collisionless electron heating mechanism is a warm plasma effect analogous to the anomalous skin effect in metals. The anomalous skin effect is a transverse analog of the Landau damping from the standpoint of wave-particle interaction in plasma [13]. The electrons gain energy through the resonant coupling with the transverse electromagnetic waves.

Although theories of collisionless heating of inductive discharges have not been well established [14–18] until now, there is some progress in understanding of the anomalous skin effect on plasma: The anomalous skin effect on the half infinite plasma was studied by Weibel [15]. In addition, the bounded plasma with a symmetric wave and, thus, current source, has been investigated by Reynolds, Blevin, and Thonemann [16] and Sayasov [19]. However their results are not directly applicable to a planar-type ICP discharge reactor, because it has current source only at one side of the plasma boundary. The modulation effect of the wave electric field by the conducting boundary at the other side of the plasma has been investigated by Yoon *et al.* [20].

However, all the above studies are only for the one-dimensional case, and a realistic current source is not included. The lack of a general heating formula, which is valid for an arbitrary chamber size, electron collisions, and the position and size of antenna coil, has hindered an accurate modeling of the plasma discharge phenomena. The first difficulty in two-dimensional modeling is that the radial normal mode of an electron kinetic equation is not amenable to cooperation with the eigenmode of the wave equation. This has been overcome in this work by assuming that the radius of the reactor chamber is sufficiently larger than the skin depth, as is the case with the usual TCP discharges. The next problem is the determination of excitation coefficients of the wave normal mode by the external coil current. The usual treatment of the wave excitation problem is based on the induction theorem [21] and the effective current sheet model [22]. However, the induction theorem originates in the uniqueness theorem of the Maxwell equations, and thus the uniqueness theorem should be assured in this case. We show that the uniqueness theorem can be proved in this problem, and that the effect of the antenna current on the plasma can be described by an effective surface current. Utilizing the Maxwell equations, the effective surface current is self-consistently determined from the real antenna current source. We present an analytic and two-dimensional solution of the anomalous skin effect in terms of the well-known conductivity of the homogeneous hot plasma and external coil current. The perfect electron reflecting boundary condition at walls is utilized to convert the finite-sized nonlocal heating problem into a periodic system with an infinite range. This equivalent infinite periodic system problem is then described by the conductivity of a homogeneous plasma and an effective current sheet. The effective current sheet is self-consistently determined from the real antenna current by manipulating the Maxwell equations. Once the electromagnetic fields are determined, then the plasma impedance can be calculated from the field quantities [23]. The resulting plasma impedance becomes a function of various parameters such as plasma density n_p, electron temperature T_e, radius of chamber R, length of plasma L_p, shielding cap length L_s, electron collision frequency ν, excitation frequency ω, and the position and size of the antenna coil. On the other hand, it was pointed out that the electron ponderomotive force can affect

*Also at Department of Physics, Korea Advanced Institute of Science and Technology, Taejeon 305-701, Korea.

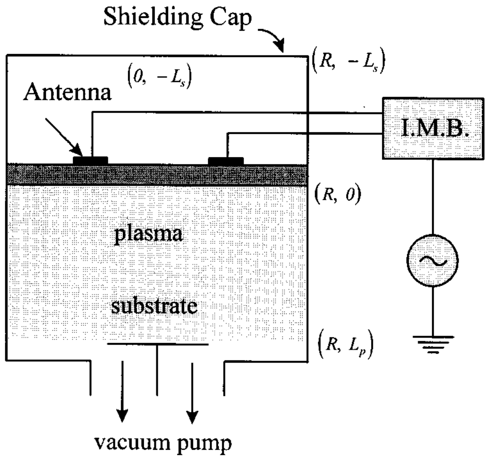

FIG. 1. Schematic diagram of the TCP reactor and the coordinate system adopted in this work.

the ambipolar diffusion in Refs. [24,25]. However the lack of an accurate calculation of the ponderomotive force has hindered an understanding of the effect of the ponderomotive force on the plasma transport. The exact calculation of the electric field in this work make possible more detailed understanding of the role of the ponderomotive force in the plasma discharge.

This paper is organized as follows. In Sec. II, the wave equation and boundary conditions are described, and the solution is presented. The numerical results for a simple antenna coil structure and discussions are presented in Sec. III. The summary of this work is given in Sec. IV. Finally, we present a mathematical verification related to the characteristic scale length of perturbed distribution, and a proof of the uniqueness theorem of the Maxwell equations in the present problem in the Appendixes.

II. THEORY

A. Maxwell-Bolzmann equations and boundary conditions

A schematic diagram of the TCP system and the coordinate system adopted in this work is presented in Fig. 1. The radio-frequency (rf) power generator is connected via a matching box to an antenna which is placed just above a dielectric plate. The time-varying magnetic-field flux induces an electric field (or equivalently, an electromotive force), and the electrons, which gain energy from the induced electric field, ionize the neutral atoms. For convenience, the whole chamber space is divided into two parts: the antenna region, which is surrounded by the shielding cap, and the plasma region.

By using Helmholz's theorem for a vector, the electric and magnetic fields can be resolved into irrotational (longitudinal or capacitive) and solenoidal (transverse or inductive) parts. Since $\nabla\cdot\mathbf{B}=0$, the magnetic field $\mathbf{B}$ is always inductive, while electric field has the inductive ($\mathbf{E}_{\rm in}$) and capacitive ($\mathbf{E}_{\rm cp}$) components. The important roles of the capacitive field are of two kinds: The first one is an active participation in the electron heating mechanism of plasma at low power. The next one is the difference between the conduction current flowing on the antenna and the input current building up the displacement current in the direction perpendicular to the antenna surface. Therefore, a self-consistent treatment of the iteration scheme, such as performed in Ref. [26], is needed to include the capacitive field effect. However, under the practical TCP discharge condition, the dominant electron heating source is still the inductive part of the electric field rather than the capacitive part, and the capacitive field is usually Faraday shielded. Therefore, only the inductive field is considered in this work.

Assuming that all physical quantities have θ symmetry, thus $\mathbf{E}_{\rm in}$, the two-dimensional wave equation describing the inductive electric field component having only a θ-component becomes

$$\nabla^2(E_\theta\boldsymbol{\theta})+\kappa^2E_\theta\boldsymbol{\theta}=\nabla^2(E_\theta)\boldsymbol{\theta}-\frac{1}{r}E_\theta\boldsymbol{\theta}+\kappa^2E_\theta\boldsymbol{\theta}$$

$$=-\frac{4\pi\omega}{c^2}iJ\boldsymbol{\theta}, \tag{1}$$

where ω is the excitation frequency, $\kappa=\omega/c$, and J is the sum of all current densities available in the reactor.

If a solution of Eq. (1) is obtained with given boundary conditions, then the magnetic field components can be estimated from

$$B_r(r,z)=\frac{i}{\kappa}\frac{\partial E_\theta(r,z)}{\partial z}, \tag{2}$$

$$B_z(r,z)=-\frac{i}{\kappa}\frac{1}{r}\frac{\partial}{\partial r}[rE_\theta(r,z)], \tag{3}$$

and the power absorbed by electrons is

$$P_{\rm abs}=\mathrm{Re}\left[\frac{1}{2}\int_V\mathbf{J}_p^*\cdot\mathbf{E}\,d\mathbf{r}\right], \tag{4}$$

where $\mathbf{J}_p$ is the plasma current density and V is the plasma volume.

All chamber wall materials are assumed to be perfect conductors, and thus $E_\theta=0$ at all chamber surfaces. There is no direct method to obtain the solution of Eq. (1) that is applicable both in antenna and plasma regions. Therefore, at first, the wave equation is solved in each region separately, and then the solutions for two regions are matched without a loss of self-consistency. An additional boundary condition is needed at the surface between the two regions. As the temporal boundary condition, let us take a $B_r(r,0)$ [or equivalently, a surface current density $K=c/4\pi B_r(r,0)$] at $z=0$. Then the solutions in each region are obtained with $B_r(r,0)$. At this time, the question of the uniqueness of the solution with this boundary condition arises. In the antenna region, it is obvious that the solution is uniquely determined with the tangential component of magnetic field [21]. However, in the plasma region, the uniqueness should be checked. We give the proof of the uniqueness of the solution in the plasma region in Appendix B. The boundary condition set is a mixed one which is generally much more difficult to handle than the normal-type problem [23]. After solving the wave equation (1) in each region, the value of $B_r(r,0)$ is determined as a function of coil current by the condition of electric field continuity at $z=0$.

B. Normal mode in the plasma region

The wave equation describing the inductive electric field in the plasma region becomes

$$\frac{\partial^2 E_\theta}{\partial r^2}+\frac{1}{r}\frac{\partial E_\theta}{\partial r}-\frac{E_\theta}{r^2}+\frac{\partial^2 E_\theta}{\partial z^2}+\kappa^2 E_\theta=-\frac{4\pi\kappa}{c}iJ_p, \quad (5)$$

where J_p is the plasma current density. As previously stated, the boundary conditions are

$$E_\theta(R,z)=0, E_\theta(r,L_p)=0 \quad \text{and}$$

$$B_r(r,0)=B_0=\frac{i}{\kappa}\left.\frac{\partial E_\theta(r,z)}{\partial z}\right|_{z=0}. \quad (6)$$

To obtain a self-consistent solution of Eq. (5), J_p should be expressed in terms of E_θ via a conductivity of plasma. With the time-varying factor $\exp(-i\omega t)$, the plasma current density can be expressed through a nonlocal conductivity of plasma Σ in general as

$$J_p(r,z)=\int_{V_p}\Sigma(r,z,r',z')E_\theta(r',z')dr'dz'. \quad (7)$$

The conductivity of plasma is to be calculated from the linearized Boltzmann equation as

$$-i\omega f_1+v_r\frac{\partial f_1}{\partial r}+v_z\frac{\partial f_1}{\partial z}+\frac{eE_\theta}{T_e}v_\theta f_0=-\nu f_1, \quad (8)$$

where the distribution function $f=f_0+f_1$, f_0 is the Maxwellian velocity distribution function, f_1 is its perturbed part, T_e is the electron temperature, ν is the collision frequency of electron with neutral atoms, and v_r, v_z, and v_θ are the r, z, and θ components of the electron velocity, respectively. Since ω is much larger than the ion plasma frequency, the ion motion is neglected.

In the typical ICP discharge condition, the term of $v_r\partial f_1/\partial r$ is much smaller than $v_z\partial f_1/\partial z$ term because

$$\frac{v_r\partial f_1/\partial r}{v_z\partial f_1/\partial z}\sim\frac{v_{th}\partial f_1/\partial r}{v_{th}\partial f_1/\partial z}\sim\frac{\delta}{R}\ll 1, \quad (9)$$

where $v_{th}=\sqrt{2T_e/m_e}$, δ is a skin depth, and m_e is the electron mass. A proof of $\partial f_1/\partial z\sim f_1/\delta$ is given in Appendix A. If the term of $v_r\partial f_1/\partial r$ is neglected in Eq. (8), the conductivity obtained from this equation is a function of only z, and the term $v_z\partial f_1/\partial z$ requires a boundary condition for the electron reflection at the walls $z=0$ and $z=L_p$. Then the current density becomes

$$J_p(r,z)=\int_0^{L_p}\Sigma(z,z')E_\theta(r,z')dz'. \quad (10)$$

As shown in the one-dimensional theory, if the perfectly reflecting boundary condition is adopted, the finite-sized problem can be converted to a periodic system problem with an infinite range along z, and the current density can be expressed with the conductivity of an infinitely homogeneous plasma. Therefore, if we neglect the term $v_r\partial f_1/\partial r$ in the linearized Bolzmann equation, and the definitions of E_θ and J_p are extended into the domains $z<0$ and $z>L_p$ in a similar manner to the one-dimensional case, the current density can be expressed with the conductivity of an infinitely homogeneous plasma as

$$J_p(r,z)=\int_{-\infty}^{\infty}\sigma(z-z')E_\theta(r,z')dz', \quad (11)$$

where $\sigma(z)$ is the one-dimensional conductivity of the homogeneous plasma, which has translational invariance along z, and its Fourier component is

$$\sigma_q\equiv\frac{1}{\sqrt{2\pi}}\int_{-\infty}^{\infty}\sigma(z)e^{-iqz}dz=-\frac{i}{\sqrt{\pi}}\frac{\omega_p}{8\pi}\frac{q_D}{q}Z_p\left(\frac{\omega+i\nu}{|q|v_{th}}\right), \quad (12)$$

where ω_p is the plasma frequency, q_D is the Debye wave number defined by $q_D=\sqrt{4\pi n_e^2/T_e}$, and Z_p is the plasma dispersion function [27] with electron density n_e. In this infinitely periodic system, the electric field is not differentiable at $z=z_n\equiv nL_p$, where n is an arbitrary integer, and thus the second derivative of E_θ do not have a finite value at these points. As in the one-dimensional case, the wave equation, which properly describes all points including the discontinuities of the derivative of E_θ, can be obtained by adding δ-function terms on the right-hand side of Eq. (5) as

$$\frac{\partial^2 E_\theta}{\partial r^2}+\frac{1}{r}\frac{\partial E_\theta}{\partial r}-\frac{E_\theta}{r^2}+\frac{\partial^2 E_\theta}{\partial z^2}+\kappa^2 E_\theta$$
$$=-\frac{4\pi\kappa}{c}iJ_p-2i\kappa\sum_{n=-\infty}^{\infty}B_r(r,z_n+0)\delta(z-z_n) \quad (13)$$

where $\delta(z)$ is the Dirac delta function, and

$$B_r(r,z_n+0)\equiv\lim_{\varepsilon\to 0}B_r(r,z_n+\varepsilon),$$

$$B_r(r,z_n-0)\equiv\lim_{\varepsilon\to 0}B_r(r,z_n-\varepsilon)=-B_r(r,z_n+0) \quad \text{for } \varepsilon\geqslant 0. \quad (14)$$

E_θ and J_p can be expanded by the Fourier-Bessel series without loss of generality as

$$E_\theta(r,z)=\sum_{m=1}^{\infty}J_1(p_m r)\left[\frac{e_{m0}^{(p)}}{2}+\sum_{n=1}^{\infty}e_{mn}^{(p)}\cos(q_n z)\right],$$

$$J_p(r,z)=\sum_{m=1}^{\infty}J_1(p_m r)\left[\frac{j_{m0}^{(p)}}{2}+\sum_{n=1}^{\infty}j_{mn}^{(p)}\cos(q_n z)\right], \quad (15)$$

where J_1 is the first-order Bessel function, $p_m\equiv\alpha_{1,m}/R$, and $q_n\equiv n\pi/L_p$, and where $\alpha_{1,m}$ is the mth zero of J_1. The Neumann function $N_n(p_m r)$ disappears in Eq. (15) in order to maintain finite values of E_θ and J_p at $r=0$. The components of the Fourier-Bessel series $e_{mn}^{(p)}$ and $j_{mn}^{(p)}$ are defined by

$$e_{mn}^{(p)}=\frac{4}{L_pR^2J_2^2(\alpha_{1,m})}\int_0^{L_p}\int_0^R E_\theta J_1(p_m r)\cos(q_n z) r\, dr\, dz,$$

$$j_{mn}^{(p)}=\frac{4}{L_pR^2J_2^2(\alpha_{1,m})}\int_0^{L_p}\int_0^R J_p J_1(p_m r)\cos(q_n z) r\, dr\, dz, \tag{16}$$

where J_2 is the second-order Bessel function. The relation between $e_{mn}^{(p)}$ and $j_{mn}^{(p)}$ is obtained from the convolution of Eq. (10) as

$$j_{mn}^{(p)}=\sqrt{2\pi}\sigma_n e_{mn}^{(p)}, \tag{17}$$

where $\sigma_n\equiv\sigma_{q_n}$. If Eqs. (15) and (17) are substituted into Eq. (13), we have

$$-(q_n^2-\kappa^2)E_\theta-\sum_{m,n} p_m^2 e_{mn}^{(p)} J_1(p_m r)\cos(q_n z)$$
$$=-\frac{4\pi\kappa}{c}iJ_p-2i\kappa\sum_{n=-\infty}^{\infty} B_r(r,z_n+0)\,\delta(z-z_n). \tag{18}$$

And, if Eq. (18) is multiplied by $\cos(q_n z)$ and integrated from $-L_p$ to L_p after being substituted into Eq. (15), we have

$$-\sum_{m=1}^{\infty}(q_n^2+p_m^2)e_{mn}^{(p)}J_1(p_m r)$$
$$=-\sqrt{2\pi}\frac{4\pi\kappa}{c}i\sigma_n\sum_{m=1}^{\infty} e_{mn}^{(p)}J_1(p_m r)$$
$$-\frac{2i\kappa}{L_p}[B_0(r)-(-1)^n B_w(r)], \tag{19}$$

with definitions of

$$B_w\equiv B_r(r,L_p-0)=-B_r(r,L_p+0). \tag{20}$$

$e_{mn}^{(p)}$ is obtained by multipling $rJ_1(p_m r)$ by Eq. (19) and by integrating from 0 to R as

$$e_{mn}^{(p)}=\frac{2i\kappa}{L_p}\frac{b_{0,m}-(-1)^n b_{w,m}}{D_{mn}}, \tag{21}$$

where $b_{0,m}$ and $b_{w,m}$ are the components of the Fourier-Bessel series of $B_0(r)$ and $B_w(r)$ defined by

$$b_{0,m}=\frac{4}{R^2J_2^2(\alpha_m)}\int_0^{L_p}\int_0^R B_0(r)J_1(p_m r) r\, dr,$$

$$b_{w,m}=\frac{4}{R^2J_2^2(\alpha_m)}\int_0^{L_p}\int_0^R B_w(r)J_1(p_m r) r\, dr, \tag{22}$$

and where

$$D_{mn}=p_m^2+q_n^2-\kappa^2-\frac{4\pi\kappa}{c}i\sqrt{2\pi}\sigma_n. \tag{23}$$

To complete the calculation, $B_w(r)$ should be evaluated in terms of $B_0(r)$. $B_w(r)$ is determined from the boundary condition $E_\theta(r,L_p)=0$ as

$$E_\theta(r,L_p)=0=\sum_{m=1}^{\infty} J_1(p_m r)\left[\frac{e_{m0}^{(p)}}{2}+\sum_{n=1}^{\infty} e_{mn}^{(p)}\right]$$
$$=-\frac{2i\kappa}{L_p}\sum_{m=1}^{\infty} J_1(p_m r)\sum_{n=0}^{\infty}\frac{(-1)^n b_{0,m}-b_{w,m}}{D_{mn}}. \tag{24}$$

If Eq. (24) is multiplied by $rJ_1(p_m r)$ and integrated from 0 to R, we have

$$b_{w,m}=b_{0,m}\frac{S_m^{(2)}}{S_m^{(1)}}, \tag{25}$$

where

$$S_m^{(1)}=\sum_{n=0}^{\infty}\frac{1}{D_{mn}},\quad S_m^{(2)}=\sum_{n=0}^{\infty}\frac{(-1)^n}{D_{mn}}. \tag{26}$$

Substituting Eq. (26) into Eq. (21), we can obtain the final form of the solution as

$$e_{mn}^{(p)}=\frac{2i\kappa}{L_p}\frac{b_{0,m}}{D_{mn}}\left[1-(-1)^n\frac{S_m^{(2)}}{S_m^{(1)}}\right]. \tag{27}$$

Here $b_{0,m}$ (or surface current density) reflects the source current.

C. Excitation of the anomalous skin effect mode by source current

To complete the calculation, $b_{0,m}$ has to be expressed as a function of the coil current density $J_c(r,z)$. If we solve the wave equation or Maxwell equations in antenna region with given B_0 as the boundary condition at $z=0$, then the value of $E_\theta(r,0)$ may be obtained as a function of J_c and B_0. Then B_0 can be determined by the condition of continuity of the electric field at $z=0$.

However, in the present work, we use a simple direct method of calculating $E_\theta(r,0)$ as a function of J_c with the boundary condition of

$$E_\theta(R,z)=0,\quad E_\theta(r,-L_s)=0\quad\text{and}$$

$$B_r(r,0)=B_0=\frac{i}{\kappa}\left.\frac{\partial E_\theta(r,z)}{\partial z}\right|_{z=0}. \tag{28}$$

A similar method is used to obtain the fields by a localized source in the wave guide [23]. First, we consider eigenmodes of the sourceless wave equation for inductive fields which obey the boundary conditions except at $z=0$:

$$\mathbf{E}_m=J_1(p_m r)\sinh[\beta_m(z+L_s)]\boldsymbol{\theta}, \tag{29}$$

$$\mathbf{B}_m=B_{r,m}\boldsymbol{r}+B_{z,m}\boldsymbol{z}, \tag{30}$$

where

$$B_{r,m}=-\frac{i}{\kappa}\left[-\frac{\partial E_m}{\partial z}+\frac{1}{r}\frac{\partial}{\partial r}(rE_m)\right]$$
$$=\frac{i}{\kappa}\beta_m J_1(p_m r)\cosh[\beta_m(z+L_s)], \quad (31)$$

$$B_{z,m}=-\frac{i}{\kappa}\frac{1}{r}\frac{\partial}{\partial r}(rE_m). \quad (32)$$

Here $\beta_m=\sqrt{p_m^2-\kappa^2}$, and β_m is a real number because the chamber radius is less than the vacuum wavelength. All $\mathbf{E}_m$ and $\mathbf{B}_m$ obviously satisfy the source-free Maxwell equations and the boundary conditions of Eq. (30), except at $z=0$. The arbitrary vacuum fields $\mathbf{E}_\theta=E_\theta\boldsymbol{\theta}$ and $\mathbf{B}=B_r\boldsymbol{r}+B_z\boldsymbol{z}$, which satisfy the boundary conditions of Eq. (28), can be expanded by $\mathbf{E}_m$ and $\mathbf{B}_m$ without loss of generality. Next we use the identity of

$$\nabla\cdot[\mathbf{E}_\theta\times\mathbf{B}_m-\mathbf{E}_m\times\mathbf{B}]=\frac{4\pi}{c}\mathbf{J}_c\cdot\mathbf{E}_m, \quad (33)$$

which follows from the source-free Maxwell equations for $\mathbf{E}_m$ and $\mathbf{B}_m$, and the Maxwell equations with the source of $\mathbf{J}_c$ satisfied with $\mathbf{E}_\theta$ and $\mathbf{B}$. Integration of Eq. (33) over the volume V_s bounded by a closed surface S leads, via the divergence theorem, to the result

$$\int_S[\mathbf{E}_\theta\times\mathbf{B}_m-\mathbf{E}_m\times\mathbf{B}]\cdot\mathbf{n}\,da=\frac{4\pi}{c}\int_{V_s}\mathbf{J}_c\cdot\mathbf{E}_m d\mathbf{r}, \quad (34)$$

where $\mathbf{n}$ is an outwardly normal direction. With the assumption of perfect conductor walls at $z=-L_s$ and $r=R$, the part of the surface integral over the shielding cap vanishes. Only the integrals over the surface at $z=0$ contribute. Hence Eq. (34) can be transformed to

$$\int_0^R[E_\theta(r,0)B_{r,m}(r,0)-E_m(r,0)B_r(0)]r\,dr$$
$$=-\frac{4\pi}{c}\int_{-L_s}^0\int_0^R J_c(r,z)E_m(r,z)r\,dr\,dz. \quad (35)$$

Since $E_\theta(r,0)$ can be expanded by the Fourier-Bessel series without loss of generality as

$$E_\theta(r,0)=\sum_{m=1}^{\infty}a_m J_1(p_m r), \quad (36)$$

and by substituting expression Eq. (36) into Eq. (35) and integrating it for r from 0 to R, we have

$$a_m=i\frac{\kappa}{\beta_m}\left[\frac{4\pi}{c}j_{c,m}^{(sh,L_s)}\operatorname{sech}(\beta L_s)-\tanh(\beta_m L_s)b_{0,m}\right], \quad (37)$$

where

$$j_{c,m}^{(sh,L_s)}\equiv\frac{2}{L_sR^2J_2^2(\alpha_{1,m})}\int_{-L_s}^0\int_0^R J_c(r,z)J_1(p_m r)$$
$$\times\sinh[\beta_m(z+L_s)]r\,dr\,dz. \quad (38)$$

Notice that the above scheme yields electric fields only at the surface at $z=0$, but this solution includes the effects of the surface current over the shielding cap and the plasma current through the boundary condition of Eq. (30). Matching the above expression for the electric field at $z=0$ with the solution of the wave equation with the source of the plasma current density, we obtain $b_{0,m}$ as

$$b_{0,m}=\frac{2\pi L_s}{c}j_{c,m}^{(sh,L_s)}\left[\sinh(\beta_m L_s)+2\frac{\beta_m}{L_p}\cosh(\beta_m L_s)S_m\right]^{-1}, \quad (39)$$

where

$$S_m=\frac{(S_m^{(1)})^2-(S_m^{(1)})^2}{S_m^{(1)}}. \quad (40)$$

Combining Eqs. (27) and (39), we have

$$e_{mn}^{(p)}=\frac{4i\pi\kappa}{L_pc^2}\frac{j_{c,m}^{(sh,L_s)}}{D_{mn}}\left[1-(-1)^n\frac{S_m^{(2)}}{S_m^{(1)}}\right]\left[\sinh(\beta_m L_s)\right.$$
$$\left.+2\frac{\beta_m}{L_p}\cosh(\beta_m L_s)S_m\right]^{-1}. \quad (41)$$

From these obtained electromagnetic fields, the impedance of plasma can be determined:

$$Z^{(p)}=-\frac{2}{|I|^2}\left(-\int_{S_p}\mathbf{S}\cdot\mathbf{n}\,da\right)$$
$$=-i\frac{\omega R^2}{4L_p}\sum_{m=1}^{\infty}J_2^2(\alpha_m)\left|\frac{b_{0m}}{I}\right|^2S_m, \quad (42)$$

where S_p denotes the interface between the plasma and antenna region, and I is the input current. If we assume that the antenna size is negligible, then we can write $J_c(r,z)=\Sigma_jI_{c,j}\delta(r-r_{c,j})\delta(z-z_{c,j})$, and, since

$$j_{c,m}^{(sh,L_s)}=\sum_j\frac{4r_{c,j}}{L_sR^2J_2^2(\alpha_m)}I_{c,j}J_1(p_mr_{c,j})\sinh[\beta_m(L_s+z_{c,j})], \quad (43)$$

the plasma impedance becomes

$$Z^{(p)}=-i\frac{16\pi^2}{c^2}\frac{\omega}{L_pR^2}\sum_{m=1}^{\infty}S_m$$
$$\times\frac{\Sigma_jr_{c,j}^2J_1^2(p_mr_{c,j})\sinh^2[\beta_m(L_s+z_c)]}{|\sinh(\beta_mL_s)+(2\beta_m/L_p)\cosh(\beta_mL_s)S_m|^2}$$
$$=Z^{(p)}(n_p,T_e,\omega,\nu,R,L_p,L_s,r_c,z_c). \quad (44)$$

The δ function assumption $J_c(r,z)=\Sigma_jI_{c,j}\delta(r-r_{c,j})\delta(z-z_{c,j})$ yields an infinite value of electric field at point (r_c,z_c), and thus the self inductance of the antenna becomes infinite. Hence if we want to calculate the total impedance of the reactor, the antenna-size should be considered. However, since the main objective of this work is to investigate the functional dependence of plasma power absorption on the

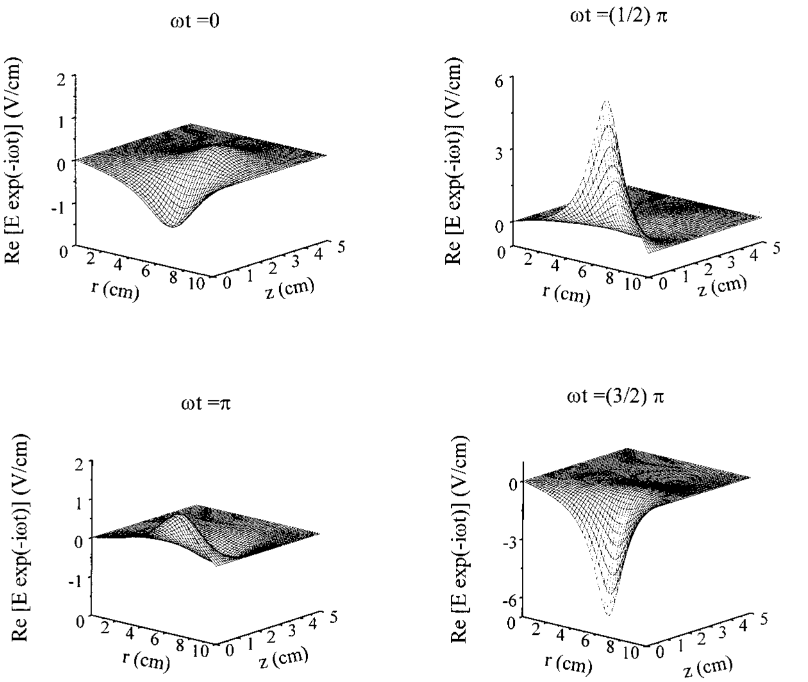

FIG. 2. Spatial variation of the electric field E at four different times of the rf period for a single-turn antenna.

various operational parameters and plasma parameters, we keep our assumption of infinitely thin antenna.

We note that the plasma impedance is a function of nine variables such as the plasma parameters n_p, T_e, and ν, the geometric parameters R, L_p, and L_s, and the antenna related parameters ω, r_c, and z_c. Although the summation on m in Eq. (44) is rapidly converging, the convergence of the sums on n in $S_m^{(1)}$ and $S_m^{(2)}$ for large m is not so good because $D_{mn} \sim p_m^2 + q_n^2$ for large n, and thus D_{mn} is not significantly increased until $q_n > p_m$. Instead of direct summations, we rearrange the summations and sum the differences between the rearranged series and their asymptotic series: If we define

$$S_m^e \equiv \frac{1}{2D_{m0}} + \sum_{n=1}^{\infty} \frac{1}{D_{m2n}}, \quad S_m^o \equiv \sum_{n=1}^{\infty} \frac{1}{D_{m2n-1}}, \tag{45}$$

then

$$S_m^{(1)} = S_m^e + S_m^o, \quad S_m^{(2)} = S_m^e - S_m^o \tag{46}$$

and asymptotic series of S_m^e and S_m^o are

$$S_m^{e,\mathrm{asp}} = \frac{1}{2\beta_m^2} + \sum_{n=1}^{\infty} \frac{1}{\beta_m^2 + q_{2n}^2} = \frac{L_p}{4\beta_m} \frac{[1+\exp(-\beta_m L_p)]^2}{1-\exp(-2\beta_m L_p)},$$

$$S_m^{o,\mathrm{asp}} = \sum_{n=1}^{\infty} \frac{1}{\beta_m^2 + q_{2n-1}^2} = \frac{L_p}{4\beta_m} \frac{[1-\exp(-\beta_m L_p)]^2}{1-\exp(-2\beta_m L_p)}. \tag{47}$$

We find that the series of the difference between S_m^e and $S_m^{e,\mathrm{asp}}$ (S_m^e and $S_m^{e,\mathrm{asp}}$) is rapidly converging.

It is interesting to compare the present $Z^{(p)}$ with its collisional case. For the limited case of $\nu \gg \omega$, it is easily shown that the collisional formula of the plasma impedance becomes

$$Z^{(p,\mathrm{col})} = -i \frac{8\pi^2}{c^2} \frac{\omega}{R^2} \sum_{m=1}^{\infty} \frac{\tanh(\gamma_m L_p)}{\gamma_m} \times \frac{\Sigma_j r_{c,j}^2 J_1^2(p_m r_{c,j}) \sinh^2[\beta_m (L_s + z_c)]}{|\sinh(\beta_m L_s) + (\beta_m/\gamma_m)\cosh(\beta_m L_s)\tanh(\gamma L_p)|^2}, \tag{48}$$

where $\gamma_m^2 = p_m^2 - \kappa^2 + (\omega_p^2/c^2)[1 + i(\nu/\omega)]^{-1}$.

The ponderomotive force potential can be calculated as

$$V_{\mathrm{pmf}} = \frac{1}{4} \frac{e^2}{m\omega^2} |E|^2. \tag{49}$$

We notice that the ponderomotive force study in the present model is not self-consistently treated, because the response of the electrons for the ponderomotive force is not included. We retain a more complete derivation of the ponderomotive force potential as a future work.

III. NUMERICAL RESULTS AND DISCUSSION

Figures 2–6 show the spatial variations of the electric field E, the magnetic-field components B_r and B_z, the plasma current density J_p, and the power density absorbed by electrons at four different times of the rf period for the case of the single-turn antenna. The default parameters in these calculations are $n_p = 10^{12}$ cm^{-3}, $T_e = 5$ eV, $\omega/2\pi = 13.56$ MHz, $\nu = 0$, $R = 10$ cm, $L_p = 5$ cm, $L_s = 10$ cm, $r_c = 7$ cm, $z_c = -1$ cm, and $I_c = 50$ A. We can see that there are minimum amplitude points for the electric and magnetic fields, and large phase changes occur at these points(Figs. 2, 3 and 4). This phenomenon is also observed in the one-dimensional theory [20], and never occurs for collisional heating with so small a chamber length relative to the vacuum wavelength of the rf wave. As expected from Max-

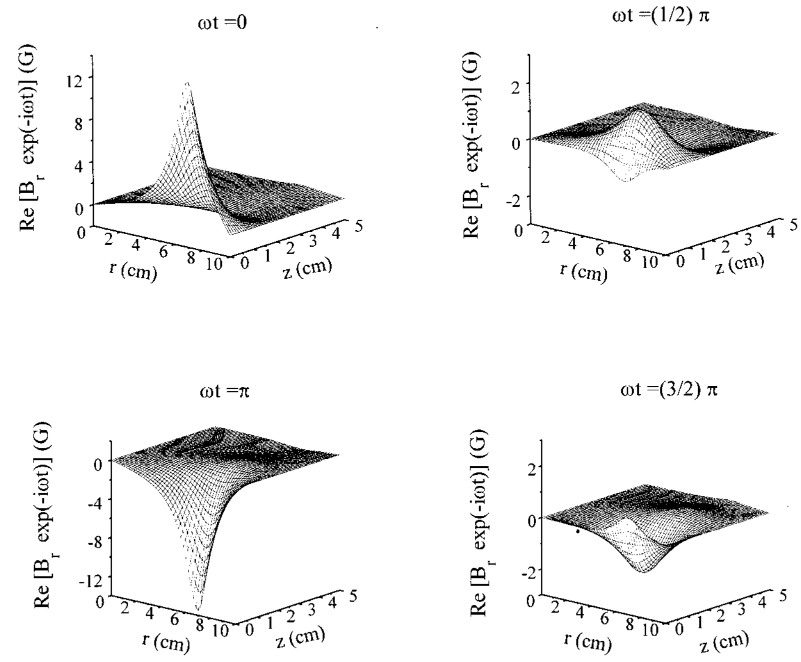

FIG. 3. Spatial variation of the magnetic-field component B_r at four different times of the rf period for a single-turn antenna.

well equations, the magnetic field is out of phase with the electric field and B_z has a node point near the antenna position (Fig. 4). Although the real part of the plasma conductivity is not zero while collision frequency is zero, the phase of the J_p is nearly out of phase with the E (Fig. 5). This is because the imaginary part of the conductivity is still greater than the real part. With this infinitely thin antenna, the deposited power density is localized near the antenna position (Fig. 6).

Figures 7–11 represent the spatial variations of the electric field E, the magnetic field components B_r and B_z, the plasma current density J_p, and the power density absorbed by electrons at four different times of the rf period for the double-turn antenna case. The default parameters are the same as in the case of a single-turn antenna, except $r_c = 4$ and 7 cm. The phase difference between the two coils of the antenna is assumed to be zero. The main features are seen to be similar to the single-turn case. Actually the conduction currents flowing on the antenna surface can be varied because there are capacitive electric field and the displacement current due to this capacitive field [26]. The investigations including the effect of the capacitive field will be the subject for our future work.

Figures 12–14 show the dependence of the plasma resis-

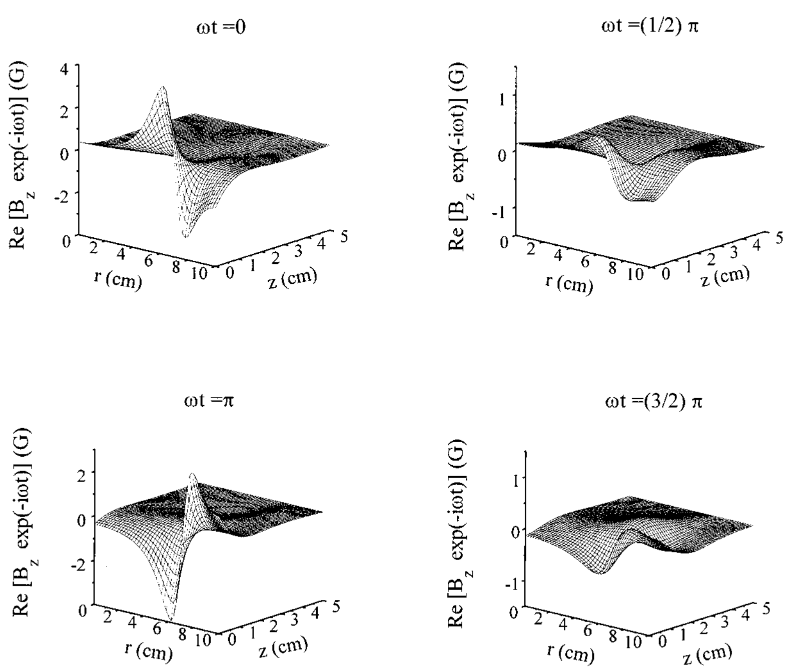

FIG. 4. Spatial variation of the magnetic-field component B_z at four different times of the rf period for a single-turn antenna.

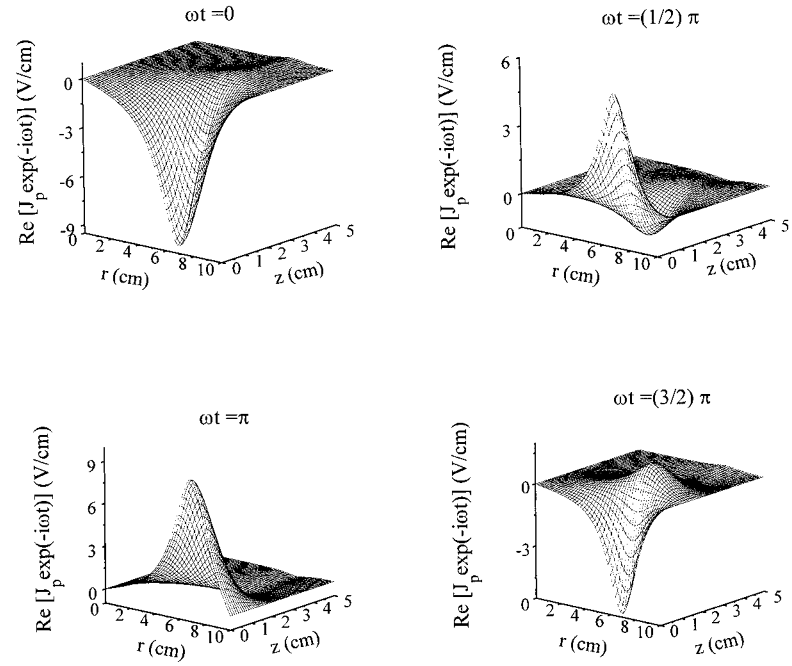

FIG. 5. Spatial variation of the plasma current density J_p at four different times of the rf period for a single-turn antenna.

tance R_p on various parameters for the single-turn antenna. The default parameters are $n_p = 10^{12}$ cm^{-3}, $T_e = 5$ eV, $\omega/2\pi = 13.56$ MHz, $\nu = 0$, $R = 10$ cm, $L_p = 20$ cm, $L_s = 10$ cm, $r_c = 7$ cm, and $z_c = -1$ cm without any specification. We notice that, in Figs. 12–14, there are some cases where the values of the parameters do not satisfy the condition $\delta \leqslant L$. In that case, the radial electron motion can change the results.

Figure 12 shows the dependence of the plasma resistance R_p on the collision frequency for different plasma densities. The dotted line is the collisional form of the real part of Eq. (48). We observe that there is a great disparity between the collisional and collisionless formulas when ν/ω is small, while the collisionless form goes over to the collisional form as ν/ω becomes large. We can also see that the larger the plasma density, the greater the disparity.

The dependence of R_p on n_p, T_e, $\omega/2\pi$, and R is represented in Fig. 13. R_p increases for the low-density region, and after meeting a maximum value it decreases as the density increases. The reason for this is similar to the case of the solenoidal-type discharge in Ref. [14], and it is as follows: In the low-density region, since the wave deeply penetrates the plasma, the skin depth δ_s is nearly equal to the chamber length, so that

$$R_p \propto \int_0^R \int_0^{L_p} \frac{|J_p|^2}{\Sigma_{\mathrm{eff}}} dz\ r\ dr, \tag{50}$$

where Σ_{eff} is the effective conductivity of plasma, and δ_s is defined by

$$\delta_s \equiv -\frac{c}{4\pi\kappa} \frac{|Z_s|^2}{\mathrm{Im}[Z_s]}, \tag{51}$$

where Z_s is the surface impedance of plasma [20]. Since the plasma current density $|J_p|^2$ is the more rapidly increasing function of n_p than Σ_{eff}, R_p is an increasing function of n_p in the low-density region. At high plasma density, since

$$R_p \propto \int_0^R \int_0^{\delta_s} \frac{|J_p|^2}{\Sigma_{\mathrm{eff}}} dz\ r\ dr \tag{52}$$

and δ_s is a decreasing function of n_p, R_p becomes a decreasing function.

R_p is an increasing function of n_p, as shown in Fig. 13(b). This is an expected result because the heating mechanism is due to the thermal effect. However, the slope has a sensitive dependence on the excitation frequency because the

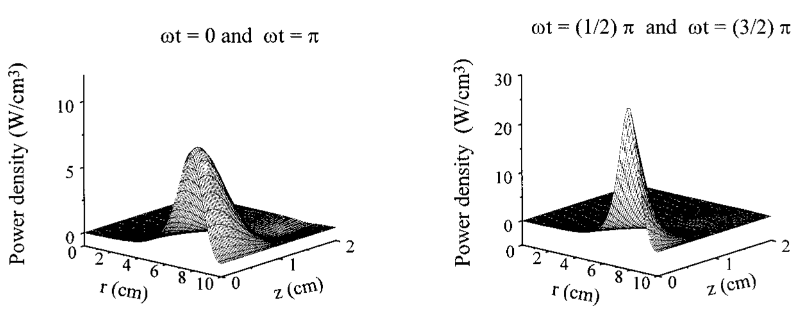

FIG. 6. Spatial variation of the absorbed power density by electrons at four different times of the rf period for a single-turn antenna.

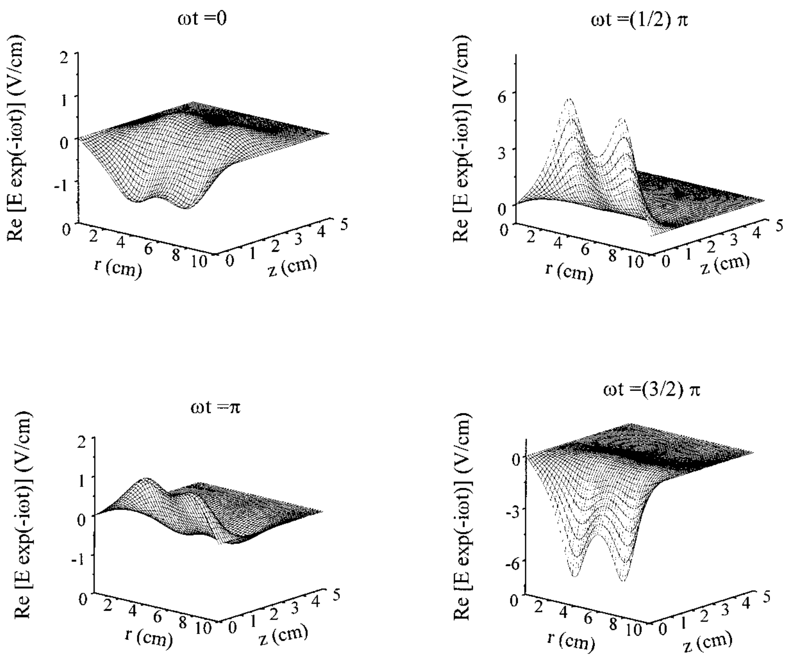

FIG. 7. Spatial variation of the electric field E at four different times of the rf period for a double-turn antenna.

wave-particle resonance is strongly related to the wave period and electron transition time [20].

Figure 13(c) shows the frequency dependence of R_p on various plasma densities. The frequency dependence of R_p is similar to the density dependence. R_p is an increasing function of the wave frequency in the low-frequency region, and becomes a decreasing function in a sufficiently high-frequency region. The reason is also quite similar to the case of the density dependence. As the wave frequency increases, the skin depth decreases, and if the skin depth becomes smaller than the chamber length, then the R_p can be expressed by Eq. (52).

If the distance between the antenna and the wall of the shielding cap is decreased, the induced current on the wall increases. Since the induced current is out of phase with the antenna current, the net current becomes small [Figs. 13(d) and 14(b)]. There is an optimum chamber length at which the resonant coupling efficiency is at a maximum [Fig. 14(a)], and this result agrees well with the result of the one-dimensional theory [20].

In Fig. 14(c), we observe that there is an optimum antenna radius for a given chamber radius. If the antenna radius increases, the induced current at the chamber wall increases. Also, if the antenna radius decreases, the flux across the antenna decreases slightly, and the induced plasma current is also reduced.

The smaller the distance between the plasma surface and antenna, the better the heating efficiency [Fig. 14(d)]. How-

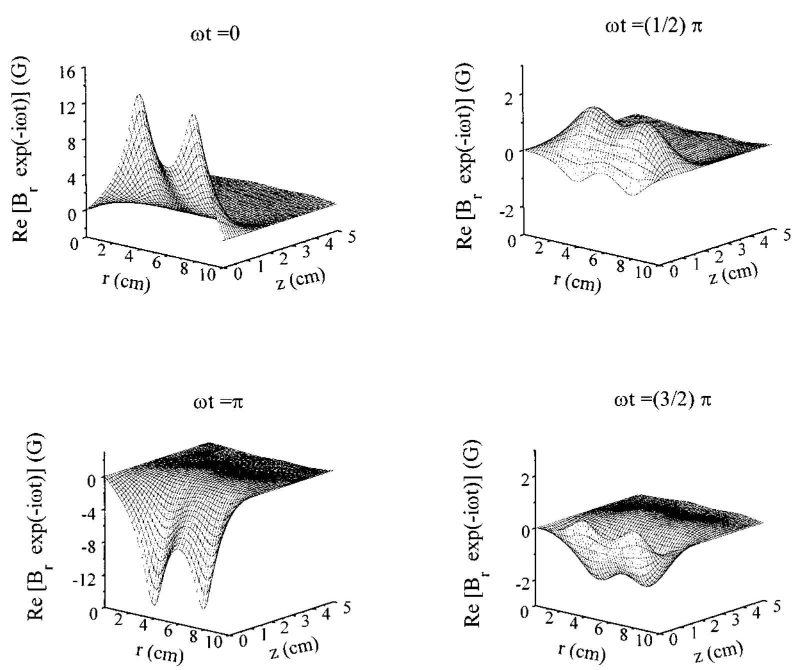

FIG. 8. Spatial variation of the magnetic-field component B_r at four different times of the rf period for a double-turn antenna.

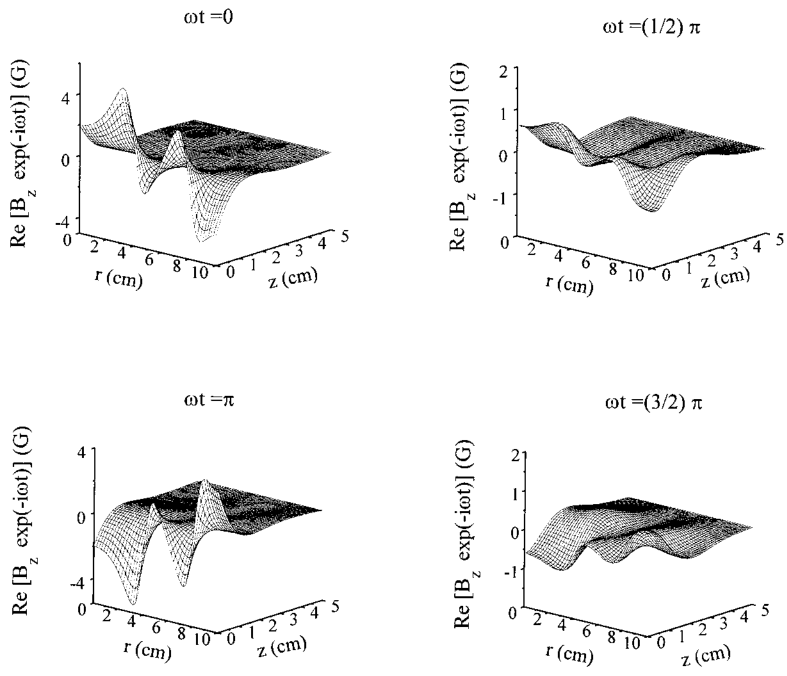

FIG. 9. Spatial variation of the magnetic-field component B_z at four different times of the rf period for a double-turn antenna.

ever, the distance is practically restricted by the width of the dielectric window.

Figure 15 represents the dependence of R_p on the phase difference between two coils for a double-turn antenna. This shows that the phase difference reduces the resistance of the plasma and also overall power absorption by the plasma. This is because the vacuum wavelength of the wave is much larger than the distance between antennas: The phase difference caused by the wave propagation along this distance is so much smaller than $\pi/2$ that there is no possibility of any constructive interference effect.

The ponderomotive force potentials V_{pmf} for the single- and double-turn cases are represented in Fig. 16. The absolute values of the V_{pmf} are several eV. This result indicates that the electron ponderomotive force can strongly affect plasma transport near the dielectric window because the presheath electric field $\sim T_e/L_p$, T_e is several eV, and the ponderomotive force per unit charge $\sim V_{\mathrm{pmf}}/\delta_s$.

IV. SUMMARY

A two-dimensional anomalous skin effect mode excitation theory of planar-type inductively coupled plasma discharge is developed. Using the calculated electromagnetic field

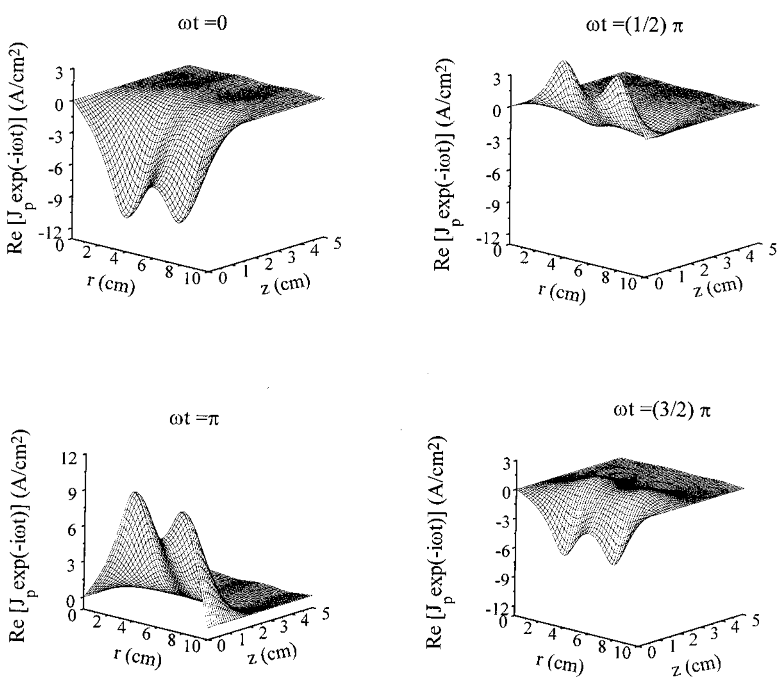

FIG. 10. Spatial variation of the plasma current density J_p at four different times of the rf period for a double-turn antenna.

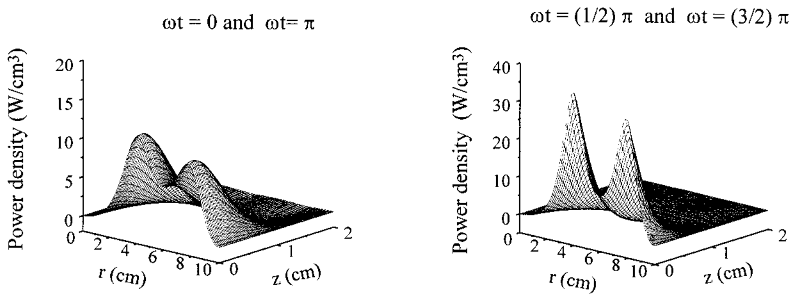

FIG. 11. Spatial variation of the absorbed power density by electrons at four different times of the rf period for a double-turn antenna.

quantities, the plasma resistance and the ponderomotive force potential are determined. The resultant plasma resistance is a function of the various discharge parameters such as the plasma density n_p, electron temperature T_e, electron collision frequency ν, radius of chamber R, length of plasma L_p, shielding cap length L_s, excitation frequency ω, and the position and size of the antenna coil. The ponderomotive force is localized at the skin depth layer, and its magnitude is sufficiently high to affect plasma transport near the dielectric window.

Although the antenna current is a directly measurable quantity, an impedance-matching network should be included for a more complete theory, and thus the antenna current should be determined self-consistently as a function of the rf power. This work requires calculations of the capacitance of the reactor and the inductance of the antenna region. These calculations are in progress, and the results will be published elsewhere.

ACKNOWLEDGMENT

This work was supported by the Ministry of Science and Technology of the Republic of Korea.

APPENDIX A

Let us consider the one-dimensional infinitely periodic system considered in Ref. [20]. It is obvious that, if $\partial J(z)/\partial z = \eta J(z)$, then $\partial f_1(z)/\partial z = \eta f_1(z)$, because

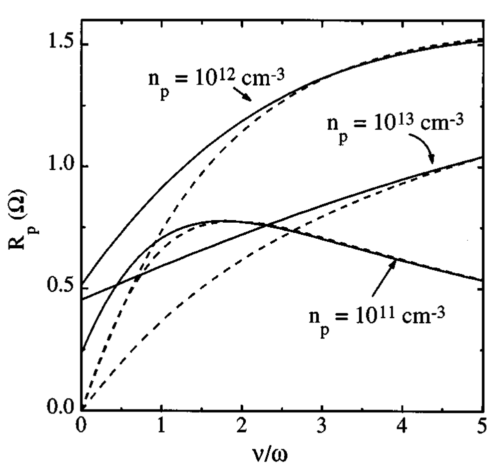

FIG. 12. Dependence of the plasma resistance R_p on the electron collision frequency ν with neutral atoms. The dotted line represents the collisional formula.

$J(z) = -en_e \int d\mathbf{v} f_1(z) v_\theta$, where $J \equiv J_\theta$ and the characteristic scale length of the electric field in the infinitely periodic system $|\eta| = \delta$. Therefore, we will show that $\partial J(z)/\partial z = \eta J(z)$ as long as $\partial E(z)/\partial z = \eta E(z)$, where $E \equiv E_\theta$. Since

$$\frac{\partial J(z)}{\partial z} = \int_{-\infty}^{\infty} \sigma(|z-z'|) E(z') dz', \tag{A1}$$

we have

$$\begin{aligned}\frac{\partial J(z)}{\partial z} &= \int_{-\infty}^{\infty} \frac{\partial \sigma(|z-z'|)}{\partial z} E(z') dz' \\ &= -\int_{-\infty}^{\infty} \frac{\partial \sigma(|z-z'|)}{\partial z'} E(z') dz' \\ &= -\sigma(|z-z'|) E(z') \Big|_{z'=-\infty}^{z'=\infty} \\ &\quad + \int_{-\infty}^{\infty} \sigma(|z-z'|) \frac{\partial E(z')}{\partial z'} dz'.\end{aligned} \tag{A2}$$

Therefore, if $\lim_{z\to\infty} \sigma(z) = 0$, then

$$\begin{aligned}\frac{\partial J(z)}{\partial z} &= \int_{-\infty}^{\infty} \sigma(|z-z'|) \frac{\partial E(z')}{\partial z'} dz' \\ &= \eta \int_{-\infty}^{\infty} \sigma(|z-z'|) E(z') dz' = \eta J(z).\end{aligned} \tag{A3}$$

Although $\lim_{z\to\infty} \sigma(z) = 0$ is physically plausible because the effect of the electric field at an infinitely long distance should be zero, we can also prove it mathematically. It is easy to show that

$$\sigma(z) = \frac{1}{\sqrt{2\pi}} \int_{-\infty}^{\infty} \sigma_q \exp(iqz) dq = \frac{m^{1/2}}{2^{5/2} \lambda_D^2} I(z), \tag{A4}$$

where λ_D^2 is the Debye length, and

$$I(l) = \int_0^{\infty} \exp\left[\frac{(-\alpha+i)l}{u} - u^2\right] \frac{du}{u}, \tag{A5}$$

where $\alpha \equiv \nu/\omega$ and $l \equiv \omega |z| / v_{\rm th}$.

First, let us consider, when $\alpha \neq 0$,

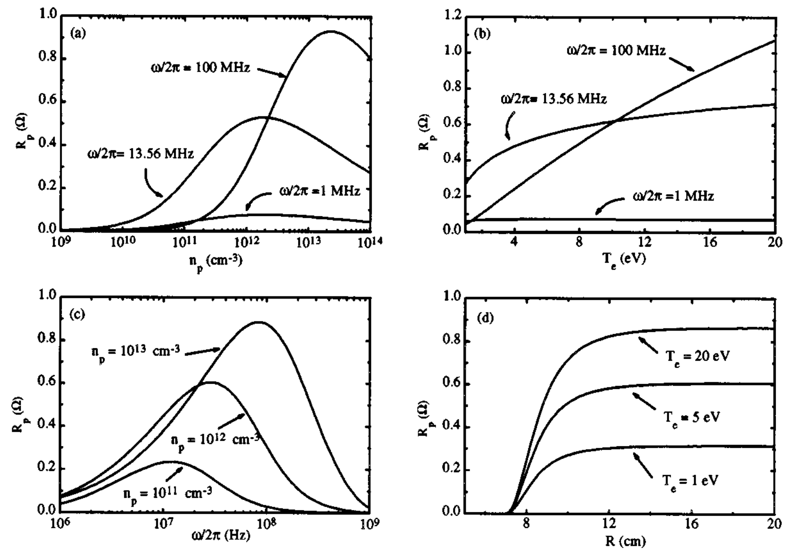

FIG. 13. Dependence of the plasma resistance R_p on n_p, T_e, $\omega/2\pi$, and R. The dotted line represents the collisional formula.

$$I(l) \leqslant \int_0^\infty \left| \exp\left[\frac{(-\alpha+i)l}{u} - u^2 \right] \right| \frac{du}{u}$$

$$= \int_0^\infty \exp\left[\frac{-\alpha l}{u} - u^2 \right] \frac{du}{u}. \tag{A6}$$

An asymptotic form of the last integration when $\alpha l \gg 1$ can be obtained by the method of steepest descent:

$$I(l) \approx \exp(-3t_0^2) \left[\frac{2\pi}{6t_0^2 - 1} \right], \quad t_0 \equiv \left(\frac{\alpha l}{2} \right)^{1/3} \quad \text{when } \alpha l \gg 1. \tag{A7}$$

From Eq. (A7), it is obvious that $\lim_{z\to\infty} I(z) = 0$ when the collision frequency is not zero.

Next, when $\alpha = 0$, let us consider

$$F(l) \equiv \int_0^\infty \exp(ilt) \frac{\exp(-1/t^2)}{t} dt. \tag{A8}$$

It can be shown that

$$F(l) = \begin{cases} I(l) & (l \geqslant 0), \\ I(l)^* & (l < 0). \end{cases} \tag{A9}$$

We have

$$F(\infty) - F(-\infty) = \lim_{l\to\infty} \int_{-l}^{l} \frac{dF(l)}{dl}$$

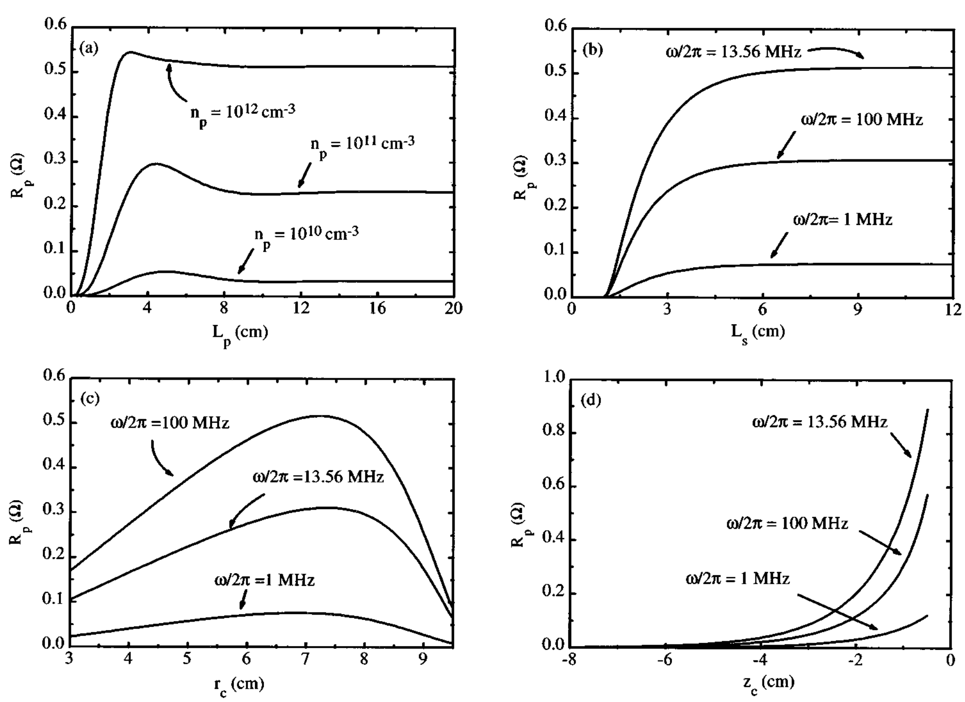

FIG. 14. Dependence of the plasma resistance R_p on L_p, L_s, r_c, and z_c. The dotted line represents the collisional formula.

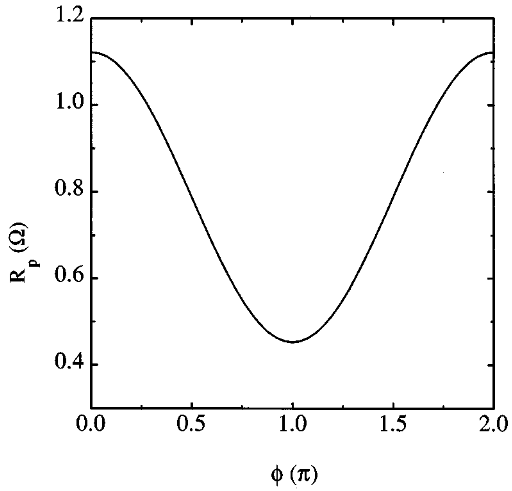

FIG. 15. Dependence of the plasma resistance R_p on the phase-different $\Delta\phi$ for a double-turn antenna.

$$=i\int_0^{\infty}\exp(-1/t^2)\lim_{l\to\infty}\left[\int_{-l}^{l}\exp(ilt)dl\right]dt$$

$$=i\sqrt{2\pi}\int_0^{\infty}\exp(-1/t^2)\,\delta(t)dt=0. \quad \text{(A10)}$$

Since

$$\lim_{t\to 0}\exp(-1/t^2)=0, \quad \text{(A11)}$$

Eq. (A10) leads us to

$$\lim_{l\to\infty}\int_0^{\infty}\sin(lt)\frac{\exp(-1/t^2)}{t}dt=0. \quad \text{(A12)}$$

Also, using the partial integration method, we can see that

$$\int_0^{\infty}\cos(lt)\,\frac{\exp(-1/t^2)}{t}dt=\frac{1}{l}\int_0^{\infty}\sin(lt)\,\frac{\exp(-1/t^2)}{t^2}\times\left(1-\frac{2}{t^2}\right)dt. \quad \text{(A13)}$$

Since

$$\lim_{t\to 0}\frac{\exp(-1/t^2)}{t}\left(1-\frac{2}{t^2}\right)=0, \quad \text{(A14)}$$

we can show similarly that

$$\lim_{l\to\infty}\int_0^{\infty}\cos(lt)\frac{\exp(-1/t^2)}{t}dt=0. \quad \text{(A15)}$$

Equations (A12) and (A15) yield

$$\lim_{l\to\infty}I(l)=0 \quad \text{when } \nu=0. \quad \text{(A16)}$$

APPENDIX B

Let us assume that the fields generated in the plasma region are $\mathbf{E}^a,\mathbf{B}^a$ and $\mathbf{E}^b,\mathbf{B}^b$. Since each set must satisfy Maxwell's equations, we have

$$\nabla\cdot\delta\mathbf{B}=0, \quad \nabla\times\delta\mathbf{E}-i\kappa\delta\mathbf{B}=0, \quad \text{(B1)}$$

$$\nabla\cdot\delta\mathbf{E}=0, \quad \nabla\times\delta\mathbf{B}-i\kappa\delta\mathbf{E}=\frac{4\pi}{c}\delta\mathbf{J}, \quad \text{(B2)}$$

where

$$\delta\mathbf{E}=\mathbf{E}^a-\mathbf{E}^b,$$

$$\delta\mathbf{B}=\mathbf{B}^a-\mathbf{B}^b,$$

$$\delta\mathbf{J}=\mathbf{J}^a-\mathbf{J}^b$$

and

$$\delta\mathbf{J}=2\pi\int_0^R\int_{-\infty}^{\infty}\sigma(\mathbf{r}-\mathbf{r}')\cdot\delta\mathbf{E}(\mathbf{r}')dz'r'dr'. \quad \text{(B3)}$$

If the tangential components of **E** or **B** are given as the boundary conditions then Eq. (B2) straightforwardly goes to the following relation:

$$\int \delta\mathbf{J}^*\cdot\delta\mathbf{E}\;d\mathbf{r}+\frac{i\omega}{4\pi}\int_V[|\delta\mathbf{E}|^2-|\delta\mathbf{E}|^2]d\mathbf{r}=0. \quad \text{(B4)}$$

Relation (B5) shows that the real part of the first term should vanish:

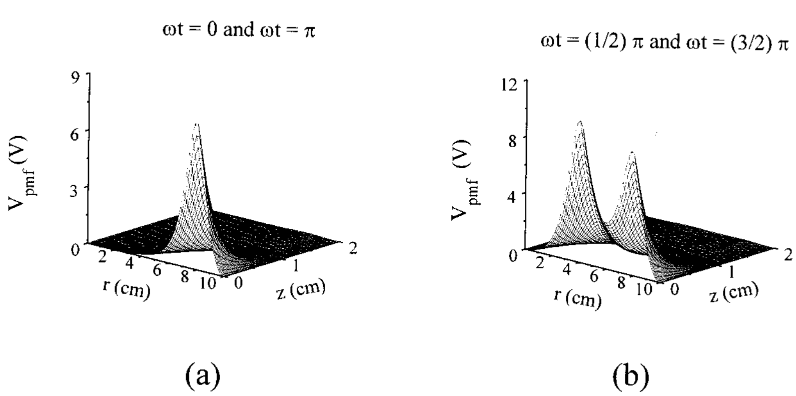

FIG. 16. Spatial variation of the ponderomotive potential $V_{\rm pmf}$ for single-turn (a) and double-turn (b) antenna cases.

$$\mathrm{Re}\left[\int \delta\mathbf{J}^{*}\cdot\delta\mathbf{E}\,d\mathbf{r}\right]=0. \tag{B5}$$

On the other hand, since the convolution relation gives

$$J(r,z)=\sqrt{2\pi}\sum_{m=1}^{\infty} J_1(p_m r)\left[\frac{\sigma_0 e_{m0}}{2}+\sum_{n=1}^{\infty} \sigma_n e_{mn}\cos(q_n z)\right], \tag{B6}$$

we have

$$\mathrm{Re}\left[\int \delta\mathbf{J}^{*}\cdot\delta\mathbf{E}\,d\mathbf{r}\right]=\frac{(2\pi)^{3/2}}{R^2 J_2^2}\sum_m \left[\frac{\mathrm{Re}[\sigma_0^{*}]|\delta e_{m0}|^2}{4}+\sum_{n=1}^{\infty} \mathrm{Re}[\sigma_n^{*}]|\delta e_{mn}|^2\right]. \tag{B7}$$

Since the sign of $\mathrm{Re}(\sigma_n^{*})$ is equal to $\mathrm{Im}(Z_p)$ and $\mathrm{Im}(Z_p)$ is always greater than zero, δe_{mn} should vanish.

[1] J. Hopwood, C. R. Guarnier, S. J. Whitehair, and J. J. Cuomo, J. Vac. Sci. Technol. A **11**, 152 (1993).

[2] J. Hopwood, C. R. Guarnier, S. J. Whitehair, and J. J. Cuomo, J. Vac. Sci. Technol. A **11**, 147 (1993).

[3] J. H. Keller, J. C. Forster, and M. S. Barnes, J. Vac. Sci. Technol. A **11**, 2487 (1993).

[4] T. Fukasawa, T. Nouda, A. Nakamura, H. Shindo, and Y. Horike, Jpn. J. Appl. Phys. **32**, 6076 (1993).

[5] P. L. G. Ventzek, T. J. Sommerer, R. J. Hoekstra, and M. J. Kushner, J. Vac. Sci. Technol. B **12**, 461 (1994).

[6] P. L. G. Ventzek, R. J. Hekstra, and M. J. Kushner, J. Vac. Sci. Technol. B **12**, 461 (1994).

[7] R. A. Stewart, P. Vitello, and D. B. Graves, J. Vac. Sci. Technol. B **12**, 478 (1994).

[8] A. P. Paranjpe, J. Vac. Sci. Technol. A **12**, 2487 (1994).

[9] G. DiPeso, V. Vahedi, D. W. Hewett, and T. D. Rognlien, J. Vac. Sci. Technol. A **12**, 2487 (1994).

[10] R. B. Piejak, V. A. Godyak, and B. M. Alexandrovich, Plasma Sources Sci. Technol. **3**, 169 (1994).

[11] D. B. Graves, IEEE Trans. Plasma Sci. **22**, 1 (1994); **22**, 31 (1994).

[12] M. M. Turner, Phys. Rev. Lett. **71**, 1844 (1993).

[13] S. Ichimaru, *Basic Principles of Plasma Physics: A Statistical Approach*, Frontiers in Physics Vol. 41 (Benjamin, Reading, MA, 1973).

[14] M. A. Lieberman and A. J. Lichtenberg, *Principles of Plasma Discharges and Materials Processing* (Wiley, New York, 1994).

[15] E. S. Weibel, Phys. Fluids, **10**, 741 (1967).

[16] J. A. Reynolds, H. A. Blevin, and P. C. Thonemann, Phys. Rev. Lett. **22**, 762 (1969).

[17] H. A. Blevin, J. A. Reynolds, and P. C. Thonemann, Phys. Fluids **13**, 1259 (1970).

[18] H. A. Blevin, J. A. Reynolds, and P. C. Thonemann, Phys. Fluids **16**, 82 (1973).

[19] Y. S. Sayasov, Helv. Phys. Acta. **52**, 288 (1979).

[20] N. S. Yoon, S. S. Kim, C. S. Chang, and D. I. Choi, Phys. Rev. E **54**, 757 (1996).

[21] C. A. Balanis, *Advanced Engineering Electromagnetics* (Wiley, New York, 1989).

[22] B. McVey, Plasma Fusion Center, Massachusetts Institute of Technology, Research Report No. PFC/RR-84-12, 1984 (unpublished).

[23] J. D. Jackson, *Classical Electrodynamics* (Wiley, New York, 1975).

[24] John C. Helmer and J. Feinstein, J. Vac. Sci. Technol. B **12**, 507 (1994).

[25] G. Dipeso, T. D. Rognlien, V. Vahedi, and D. W. Hewett, IEEE Trans. Plasma Sci. **23**, 4 (1995); **23**, 550 (1995).

[26] E. F. Jaeger, L. A. Berry, J. S. Tolliver, and D. B. Batchelor, Phys. Plasmas **2**, 2597 (1995).

[27] B. D. Fried and S. D. Conte, *The Plasma Dispersion Function* (Academic, New York, 1961).